

Direct evidence for intermediate multiferroic phase in $\text{LiCuFe}_2(\text{VO}_4)_3$

Xiyu Chen,^{1,#} Shuhan Zheng,^{1,#} Meifeng Liu,^{1,*} Tao Zou,² Wei Wang,³ Keer Nie,¹ Fei Liu,¹
Yunlong Xie,¹ Min Zeng,³ Xiuzhang Wang,¹ Hong Li,¹ Shuai Dong,^{4,*} Jun-Ming Liu^{1,5}

¹*Institute for Advanced Materials, Hubei Normal University, Huangshi 435002, China*

²*Collaborative Innovation Center of Light Manipulations and Applications, Shandong Normal University, Jinan 250358, China*

³*Institute for Advanced Materials, South China Academy of Advanced Optoelectronics, South China Normal University, Guangzhou 510006, China*

⁴*School of Physics, Southeast University, Nanjing 211189, China*

⁵*Laboratory of Solid State Microstructures, Nanjing University, Nanjing 210093, China*

ABSTRACT:

Magnetic susceptibility, specific heat, dielectric, and electric polarization of $\text{LiCuFe}_2(\text{VO}_4)_3$ have been investigated. Two sequential antiferromagnetic transitions at $T_{N1} \sim 9.95$ K and $T_{N2} \sim 8.17$ K are observed under zero magnetic field. While a dielectric peak at T_{N1} is clearly identified, the measured pyroelectric current also exhibits a sharp peak at T_{N1} , implying the magnetically relevant ferroelectricity. Interestingly, another pyroelectric peak around T_{N2} with opposite signal is observed, resulting in the disappearance of electric polarization below T_{N2} . Besides, the electric polarization is significantly suppressed in response to external magnetic field, evidencing remarkable magnetoelectric effect. These results suggest the essential relevance of the magnetic structure with the ferroelectricity in $\text{LiCuFe}_2(\text{VO}_4)_3$, deserving for further investigation of the underlying mechanism.

The two authors contribute equally to this work.

* Corresponding authors. Email: lmfeng1107@hbnu.edu.cn (Meifeng Liu), sdong@seu.edu.cn (Shuai Dong)

I. INTRODUCTION

The exploration and synthesis of novel multiferroics have been one of the major interests in condensed matter physics. In multiferroics, magnetism and ferroelectricity coexist, which allows the control of magnetization M by electric field E or electrical polarization P by magnetic field H .¹⁻⁷ Therefore, multiferroics have huge potential applications in novel electronic devices, such as memories, sensors, etc.^{4, 8} Depending on the origin of ferroelectricity, multiferroics are distinguished into two types.^{1, 9} In type-I multiferroics, the magnetism and ferroelectricity have distinctly different origins, and the magnetoelectric (ME) coupling is usually weak. For type-II multiferroics, polarization P is generated by specific magnetic structures, leading to strong ME effect. Now it is well known that the ferroelectricity in type-II multiferroics originates from spin-orbit coupling or spin-lattice coupling.^{1, 3} For instance, the ferroelectricity in TbMnO_3 and $\text{Ba}_2\text{XGe}_2\text{O}_7$ ($X = \text{Mn, Co, and Cu}$) is induced by inverse Dzyaloshinskii-Moriya interaction and spin-dependent p - d hybridization respectively.¹⁰⁻¹² These materials have non-collinear spin orders and the spin-orbit coupling dominates. Besides, in materials such as $\text{Ca}_3\text{CoMnO}_6$, the P is induced by exchange striction effect in collinear up-up-down-down spin order, which is dominated by spin-lattice coupling.^{13, 14} It is noted that these couplings belong to high order quantum effect and the induced P is usually small. Even worse, the magnetic ordering temperature in type-II multiferroics is usually low. Therefore currently available multiferroics are not suitable for application yet. Continuous efforts have been paid to explore novel materials, such as $\text{CaMn}_7\text{O}_{12}$, $\text{BiMn}_3\text{Cr}_4\text{O}_{12}$, etc.¹⁵⁻¹⁸ However, the difficulties remain, and searching for new multiferroic is still a major issue in this area.

Frustrated quasi-one-dimensional (quasi-1D) antiferromagnets have received widespread interest due to the rich and largely unexplored physics, such as quantum criticality,^{19, 20} H -induced magnetic ordering,²¹ quantum spin liquid,²² etc. Owing to the highly frustrated magnetic interactions, multiferroicity induced by non-collinear spin order is expected in quasi-1D magnetic systems. In fact, this issue has been explored in quasi-1D systems such as Cu-base quantum spin chain LiCu_2O_2 ²³ and LiCuVO_4 ,²⁴ pyroxene $\text{NaFeGe}_2\text{O}_6$ ²⁵ and $\text{SrMnGe}_2\text{O}_6$,²⁶ and zigzag chain MnWO_4 .²⁷ In these materials, strong ME effect, such as H

switching P , has been extensively investigated. Considering the large number of quasi-1D materials, it is valuable to explore further the quasi-1D magnetic systems, addressing the multiferroicity.

From this perspective, a recently reported quasi-1D mixed spin chain triple vanadate $\text{LiCuFe}_2(\text{VO}_4)_3$ attracted research interests in the multiferroic community. $\text{LiCuFe}_2(\text{VO}_4)_3$ was first synthesized by Belik,²⁸ and its crystal structure is shown in Figure 1(a-b). Neighboring FeO_6 octahedra and CuO_5 triangular bipyramids are connected by edge-sharing and form quasi-1D $\text{Cu}^{2+}\text{-Fe}^{3+}$ mixed spin chains. According to earlier work, the frustration factor $f = |\theta_{\text{CW}}|/T_{\text{N}}$ for $\text{LiCuFe}_2(\text{VO}_4)_3$ is 12, where θ_{CW} is the Curie-Weiss constant and T_{N} is the magnetic ordering temperature,²⁹ suggesting highly frustrated spin structure in $\text{LiCuFe}_2(\text{VO}_4)_3$. Besides, the first-principles calculation indicated the competition of ferromagnetic (FM) and antiferromagnetic (AFM) exchanges, which may lead to a non-collinear spin order and induce ferroelectricity.³⁰ Very recently, indirect evidences in terms of ferroelectricity and ME effect in $\text{LiCuFe}_2(\text{VO}_4)_3$ were reported,^{30,31} while direct measurement of polarization P is absent.

In this work, we present a comprehensive study of $\text{LiCuFe}_2(\text{VO}_4)_3$ including the magnetic susceptibility, specific heat, and electric polarization measurements. It will be revealed that $\text{LiCuFe}_2(\text{VO}_4)_3$ undergoes two successive AFM transitions at $T_{\text{N}1} \sim 9.95$ K and $T_{\text{N}2} \sim 8.17$ K, as evidenced by magnetic susceptibility and specific heat. Very interestingly, two sign-opposite pyroelectric peaks at $T_{\text{N}1}$ and $T_{\text{N}2}$, marking the generation and disappearing of polarization P respectively are identified. The ME effect in terms of varying polarization P under different H is also presented.

II. EXPERIMENT

Polycrystalline samples of $\text{LiCuFe}_2(\text{VO}_4)_3$ were synthesized by the conventional solid-state reaction method. The stoichiometric mixtures of Li_2CO_3 , CuO , Fe_2O_3 , and V_2O_5 were sufficiently ground and fired at 600 °C for 24 hours in air. The obtained powders were reground and pelleted. Then, the resultant pellets were sintered at 640 °C for 72 hours in air again with three intermediate regrinding and pelleting processes. Eventually, the phase purity of powder samples were analyzed using an X-ray diffractometer (SmartLab Se, Rigaku) with

Cu- $K\alpha$ radiation at room temperature (T).

The dc magnetic susceptibility $\chi(T)$ as a function of T under different magnetic fields H was measured using Physical Property Measurement System (PPMS DynaCool-9, Quantum Design). The specific heat (C_p) was also measured in PPMS DynaCool-9 based on the heat relaxation method.

For electrical measurement, Au electrodes were deposited on the top and bottom sides of the disk-like sample (3.25 mm in diameter and 0.3 mm in thickness). The measurements were carried out in PPMS which provides magnetic field and cryogenic environment. The dielectric constant ϵ_r was measured by an LCR meter (Agilent E4980A). For pyroelectric current (I_{pyro}) measurement, the poling electric field E_p was provided by Keithley 6517B electrometer. Before the measurement, the sample was cooled from 15 K to 2 K under $E_p = \pm 3.33$ kV/cm. When the sample temperature was cooled to 2 K, the poling electric field was removed and the sample was short-circuited for 30 minutes to remove the trapped charge. Then the pyroelectric current was recorded using the Keithley 6517B electrometer when raising the temperature. The P is derived by integrating the pyroelectric current. It is noted that the magnetic field remained unchanged during the pyroelectric measurement.

III. RESULTS

Figure 1c displays the measured X-ray spectrum of $\text{LiCuFe}_2(\text{VO}_4)_3$ powders. No stray peaks are identified, suggesting the high purity of $\text{LiCuFe}_2(\text{VO}_4)_3$. The diffraction patterns are further analyzed by Rietveld refinement.^{32, 33} The space group of $\text{LiCuFe}_2(\text{VO}_4)_3$ is fitted to be triclinic $P-1$, and the refined structure parameters are $a = 8.1457(99)$ Å, $b = 9.8032(82)$ Å, $c = 6.6334(72)$ Å, $\alpha = 103.825(3)^\circ$, $\beta = 102.361(0)^\circ$, $\gamma = 106.992(4)^\circ$. The results are consistent with earlier reports.²⁹⁻³¹ More detailed structural parameters are displayed in Table I.

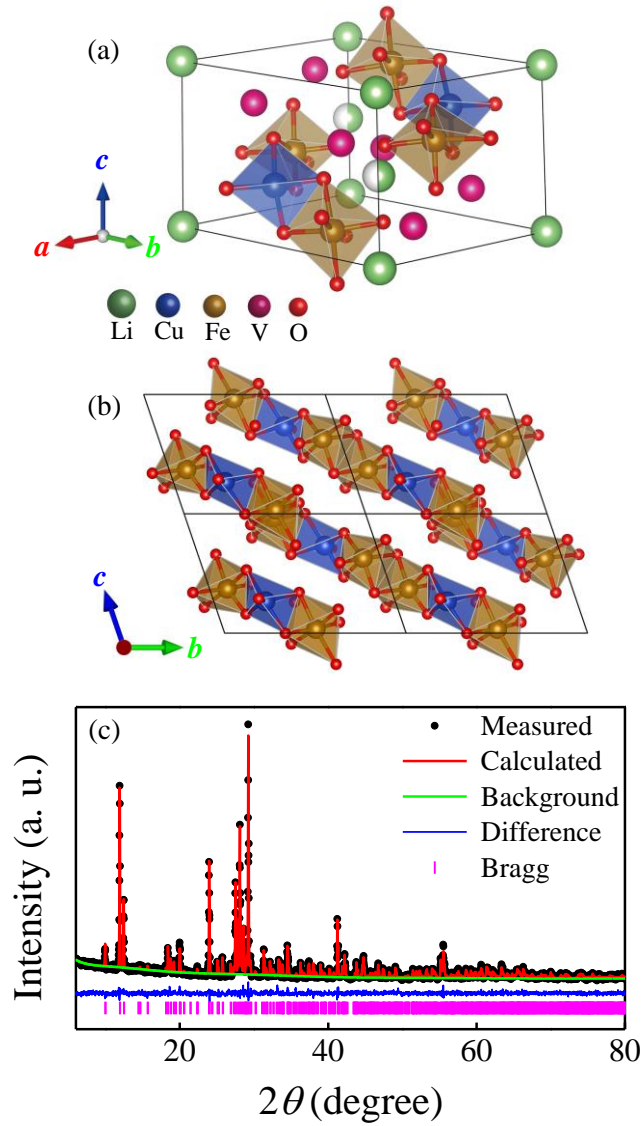


Figure 1. (a-b) Schematic of the crystal structure of $\text{LiCuFe}_2(\text{VO}_4)_3$. The unit cells are indicated by black boxes. (c) Rietveld refined powder X-ray spectrum of $\text{LiCuFe}_2(\text{VO}_4)_3$ at room temperature.

Table I. Refined structure information of $\text{LiCuFe}_2(\text{VO}_4)_3$ from powder X-ray diffraction at room T

| Atom (Wyck.) | x | y | z | Occ. | Site |
|--------------|-----------|-----------|-----------|-------|------|
| Li1 | 0.0000 | 0.0000 | 0.0000 | 1.000 | 1a |
| Li2 | 0.0909(3) | 0.0743(0) | 0.5118(5) | 0.500 | 2i |
| Cu1 | 0.7780(0) | 0.2847(5) | 0.2667(9) | 1.000 | 2i |
| Fe1 | 0.4493(7) | 0.0969(3) | 0.3716(1) | 1.000 | 2i |
| Fe2 | 0.6990(2) | 0.5106(4) | 0.0343(0) | 1.000 | 2i |
| V1 | 0.6015(6) | 0.8320(9) | 0.1164(9) | 1.000 | 2i |

| | | | | | |
|-----|------------|------------|------------|-------|----|
| V2 | 0.2257(7) | 0.3740(1) | 0.4082(9) | 1.000 | 2i |
| V3 | 0.1565(2) | 0.7601(0) | 0.2336(9) | 1.000 | 2i |
| O1 | 0.0205(0) | 0.2524(2) | 0.2885(2) | 1.000 | 2i |
| O2 | 0.5446(5) | -0.0985(6) | 0.3396(7) | 1.000 | 2i |
| O3 | 0.2700(4) | 0.4442(0) | 0.2607(5) | 1.000 | 2i |
| O4 | 0.3175(1) | 0.2325(2) | 0.4085(1) | 1.000 | 2i |
| O5 | 0.2700(7) | 0.7617(8) | 0.4707(5) | 1.000 | 2i |
| O6 | 0.5658(9) | 0.6527(0) | 0.0913(7) | 1.000 | 2i |
| O7 | 0.8239(9) | -0.0968(7) | 0.1619(6) | 1.000 | 2i |
| O8 | 0.5070(1) | 0.1539(7) | 0.1606(1) | 1.000 | 2i |
| O9 | 0.7816(0) | 0.3336(8) | -0.0018(1) | 1.000 | 2i |
| O10 | 0.7187(0) | 0.4874(9) | 0.3396(7) | 1.000 | 2i |
| O11 | 0.1921(9) | -0.0632(8) | 0.2165(8) | 1.000 | 2i |
| O12 | -0.0562(6) | 0.6712(0) | 0.1997(9) | 1.000 | 2i |

Space group: $P-1$, $a = 8.1457(99)$ Å, $b = 9.8032(82)$ Å, $c = 6.6334(72)$ Å, $\alpha = 103.825(3)^\circ$, $\beta = 102.361(0)^\circ$, $\gamma = 106.992(4)^\circ$, $R_p = 3.04\%$, $R_{wp} = 3.89\%$, $\chi^2 = 1.121$

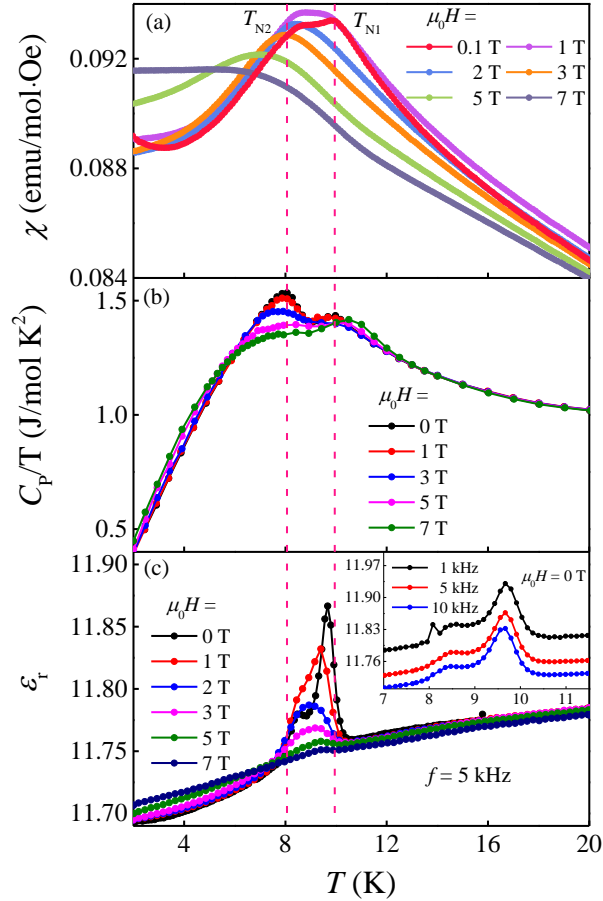


Figure 2. (a) T -dependent magnetic susceptibility under different H . (b) T -dependent C_p/T of $\text{LiCuFe}_2(\text{VO}_4)_3$ under different H . (c) The dielectric constant ϵ_r under different H with $f = 5$ kHz. The inset shows the T dependence of ϵ_r with various frequencies under zero H .

Figure 2a shows the magnetic susceptibility χ as a function of temperature measured at various magnetic field H . Two anomalies are found at $T_{N1} \sim 9.9$ K and $T_{N2} \sim 8.6$ K under $\mu_0 H = 0.1$ T, indicating the onset of long-range magnetic ordering (LRO). With increasing H , the peaks of $\chi(T)$ slowly drift to lower T and become broader. This suggests that the LRO of $\text{LiCuFe}_2(\text{VO}_4)_3$ is suppressed by H , which is a typical behavior of AFM system.^{34, 35} To further check the magnetic transition of $\text{LiCuFe}_2(\text{VO}_4)_3$, we measured the specific heat C_p of $\text{LiCuFe}_2(\text{VO}_4)_3$ under different H . Similarly, the C_p/T of $\text{LiCuFe}_2(\text{VO}_4)_3$ under zero H exhibits two serial peaks at $T_{N1} \sim 9.95$ K and $T_{N2} \sim 8.17$ K, as shown in Figure 2b. With increasing H , the peak at T_{N2} drifts to lower T and is suppressed. The specific heat measurement verifies that the AFM transitions of $\text{LiCuFe}_2(\text{VO}_4)_3$ are suppressed by H , which is consistent with $\chi(T)$ curves.

As to the electrical measurements, the dielectric constants $\epsilon_r(T)$ is measured first, as presented in Figure 2c. The $\epsilon_r(T)$ exhibits a sharp peak at T_{N1} and a step-like anomaly at T_{N2} under zero H , as shown in the inset of Figure 2c. These two anomalies do not shift with increasing measuring frequency, ruling out the possibility of artifactual signal from defects' relaxation. Then the magneto-dielectric effect is investigated. As shown in Figure 2c, the two anomalies are significantly suppressed and drift to lower T with increasing H . And the anomalies are almost unrecognizable at $\mu_0 H = 7$ T. These results are consistent with $\chi(T)$ and C_p data. The remarkable magneto-dielectric effect hints the existence of ferroelectricity and remarkable ME effect. Actually, previous studies have claimed the multiferroicity of $\text{LiCuFe}_2(\text{VO}_4)_3$ by discussing the dielectric signals,^{30, 31} but the direct ferroelectric measurements are still missing.

The pyroelectric current $I_{\text{pyro}}(T)$ is measured to reveal the electrical polarization of $\text{LiCuFe}_2(\text{VO}_4)_3$. Figure 3a shows $I_{\text{pyro}}(T)$ of $\text{LiCuFe}_2(\text{VO}_4)_3$ obtained at various heating rates (2, 4, and 6 K/min) under poling electric field $E_p = 3.33$ kV/cm and zero magnetic field. Interestingly, two current peaks with opposite directions are observed at T_{N1} and T_{N2} respectively. The current peaks are un-shifted with various heating rates, indicating that the current signals are indeed from pyroelectric effect. Besides, the poling with a negative electric field indeed leads to a reversal of $I_{\text{pyro}}(T)$, as demonstrated in Figure 3a. Figure 3b presents the

$P(T)$ curves obtained by integrating the $I_{\text{pyro}}(T)$. The $P(T)$ curves measured under $\pm E_p$ have similar magnitude with opposite directions, implying that the P can be reversed and thus $\text{LiCuFe}_2(\text{VO}_4)_3$ is indeed a ferroelectric material. In short, through the combination of $\chi(T)$, C_p , ϵ_r , and $I_{\text{pyro}}(T)$ measurements, we exhibit the simultaneous existence of FE transition and AFM transitions, and confirm that $\text{LiCuFe}_2(\text{VO}_4)_3$ is a magnetically induced multiferroics (i.e., a type-II multiferroic one).

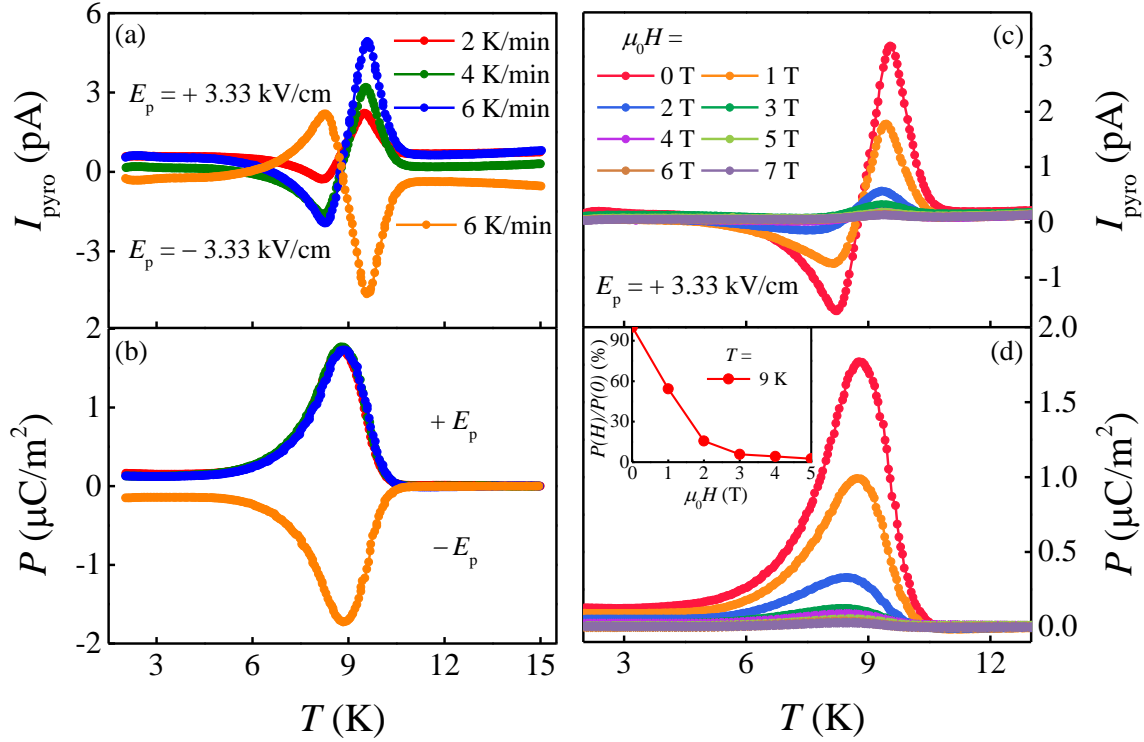


Figure 3. (a) The pyroelectric current of $\text{LiCuFe}_2(\text{VO}_4)_3$ measured at various heating rates: 2 K/min, 4 K/min, and 6 K/min under $E_p = \pm 3.33$ kV/cm and $\mu_0H = 0$ T. (b) The T -dependent ferroelectric polarization derived by integrating the pyroelectric current relative to time under $E_p = \pm 3.33$ kV/cm and $\mu_0H = 0$ T. (c) The pyroelectric current and (d) the corresponding ferroelectric polarization of $\text{LiCuFe}_2(\text{VO}_4)_3$ under various H and $E_p = \pm 3.33$ kV/cm. Insert: ME effect at $T = 9$ K.

Then the ME effect of $\text{LiCuFe}_2(\text{VO}_4)_3$ can be demonstrated by measuring the $I_{\text{pyro}}(T)$ curves under different H , and the results are presented in Figure 3c. With increasing H , the two pyroelectric current peaks slightly shift to lower T and the magnitudes decrease

simultaneously. It is noted that the pyroelectric current is too weak to be recognized when H is higher than 3 T. Figure 3d depicts the P under different H , which is significantly suppressed by increasing H . Such behavior is widely observed in many type-II multiferroics, which further suggests that $\text{LiCuFe}_2(\text{VO}_4)_3$ is one of the cases.^{13, 36}

IV. DISCUSSION

According to above measurements, it is obvious that $\text{LiCuFe}_2(\text{VO}_4)_3$ belongs to the type-II multiferroics. On one hand, complicated magnetic interactions were argued to exist between Fe-Cu and Fe-Fe spins in $\text{LiCuFe}_2(\text{VO}_4)_3$,^{29, 30} which might lead to frustrated spin states like non-collinear spin texture with incommensurate/commensurate period. On the other hand, the P of $\text{LiCuFe}_2(\text{VO}_4)_3$ is highly susceptible to H , which can be attributed to the change of spin texture upon H . Both these characteristics are feature of type-II multiferroics. Besides these common characteristics, the multiferroicity in $\text{LiCuFe}_2(\text{VO}_4)_3$ is special for its two pyroelectric current peaks. There are two possibilities to explain this nontrivial behavior.

The first possibility is that these two peaks could be from two independent ferroelectric components with different transition points, like recently proposed “irreducible ferrielectricity”.³⁷ In $\text{LiCuFe}_2(\text{VO}_4)_3$, there are two different magnetic ions (Cu^{2+} and Fe^{3+}) and Fe^{3+} ions have two nonequivalent positions. Therefore these Cu^{2+} and Fe^{3+} ions may order in different temperatures, and form two different sublattices which contribute to the net P independently. Similar scenario can be referred to extensively researched RMn_2O_5 ³⁸⁻⁴⁰ and DyMnO_3 .^{41, 42} In RMn_2O_5 two ferroelectric components are identified, which originate from $\text{Mn}^{3+}\text{-Mn}^{4+}\text{-Mn}^{3+}$ blocks and $\text{R}^{3+}\text{-Mn}^{4+}\text{-R}^{3+}$ blocks respectively.^{43, 44} In DyMnO_3 , the Mn sublattice and Dy sublattice orders in different temperatures, and contribute to the net polarization in opposite directions.^{41, 42}

The second possibility is that the two current peaks correspond to sequential magnetic transitions. Before T_{N1} , the paramagnetic phase is nonpolar, and the AFM phase below T_{N2} is also nonpolar. Only the AFM phase between T_{N1} and T_{N2} breaks the spatial inversion symmetry and generates the polarization. Such scenario of intermediate multiferroic phases have also been found in MnWO_4 , $\text{Ni}_3\text{V}_2\text{O}_8$, and CuO .^{27, 45-50} In these materials, multiple

magnetic transitions take place at different temperature and the ferroelectricity only exists in the temperature windows of incommensurate magnetic structures.^{27, 45-48}

According to above discussions, the complicated magnetic interaction in $\text{LiCuFe}_2(\text{VO}_4)_3$ makes the presence of two sequential magnetic transitions. Thus, the second scenario seems to be much more likely than the first one. To further verify this scenario, the sample was cooled down to 2 K without poling electric field, and then poled the sample from 2 K to 9 K with an electric field $E = \pm 3.33$ kV/cm. Then, the pyroelectric current of $\text{LiCuFe}_2(\text{VO}_4)_3$ was measured during the heating or cooling the samples. As shown in Figure 4a, the ferroelectric polarization P only exists between T_{N2} and T_{N1} , while it is negligible in other region. Besides, this P is identical to the case with poling from 20 K to 9 K, as compared in Figure 4b. Hence, we are confident that $\text{LiCuFe}_2(\text{VO}_4)_3$ is similar to CuO, which belongs to the family of intermediate multiferroic systems. Of course, the magnetic structure of $\text{LiCuFe}_2(\text{VO}_4)_3$ has not been resolved yet. In future, neutron diffraction experiments are desired to clarify this issue by solving the magnetic structures of $\text{LiCuFe}_2(\text{VO}_4)_3$ between T_{N1} and T_{N2} , as well as below T_{N2} .

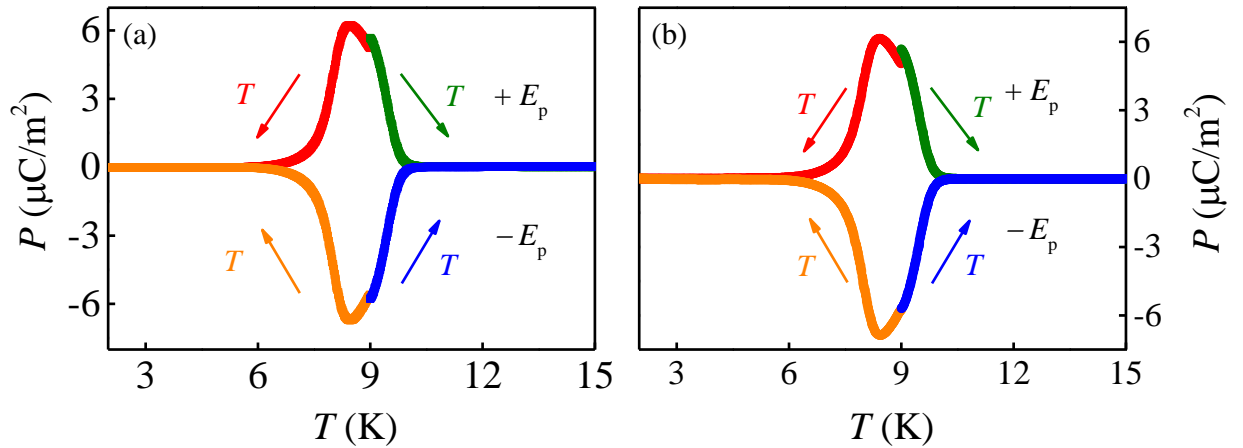


Figure 4. The ferroelectric polarization of $\text{LiCuFe}_2(\text{VO}_4)_3$. The corresponding pyroelectric current was measured when cooling the sample from 9 K to 2 K (red and orange) or heating the sample from 9 K to 15K (green and blue). (a) With a poling process from 2 K to 9 K. (b) With a poling process from 20 K to 9 K. The poling field is fixed as $E_p = \pm 3.33$ kV/cm.

Based on the second scenario, the magnetic and polar phase diagram for $\text{LiCuFe}_2(\text{VO}_4)_3$ is plotted in Figure 5, according to above measurements. It is paramagnetic (PM) and paraelectric (PE) above $T_{N1} \sim 9.95$ K. When the T decreases to T_{N1} , $\text{LiCuFe}_2(\text{VO}_4)_3$ undergoes the first AFM phase transition (so called AFM1 phase), and simultaneously a ferroelectric phase transition (FE phase) occurs at T_{N1} . As T further decreases, another AFM transition (so called AFM2 phase) occurs at $T_{N2} \sim 8.17$ K. The AFM2 phase transition leads to the disappearance of ferroelectricity. Therefore $\text{LiCuFe}_2(\text{VO}_4)_3$ is marked as paraelectric below T_{N2} . The applied magnetic field can slightly expand this multiferroic window. Under the magnetic field, the anomaly signal can slightly broaden the ferroelectric phase region, which may be related to possible frustrated spin structure. Maybe the magnetic field can suppress the frustration, which enhances the ordering temperature slightly.

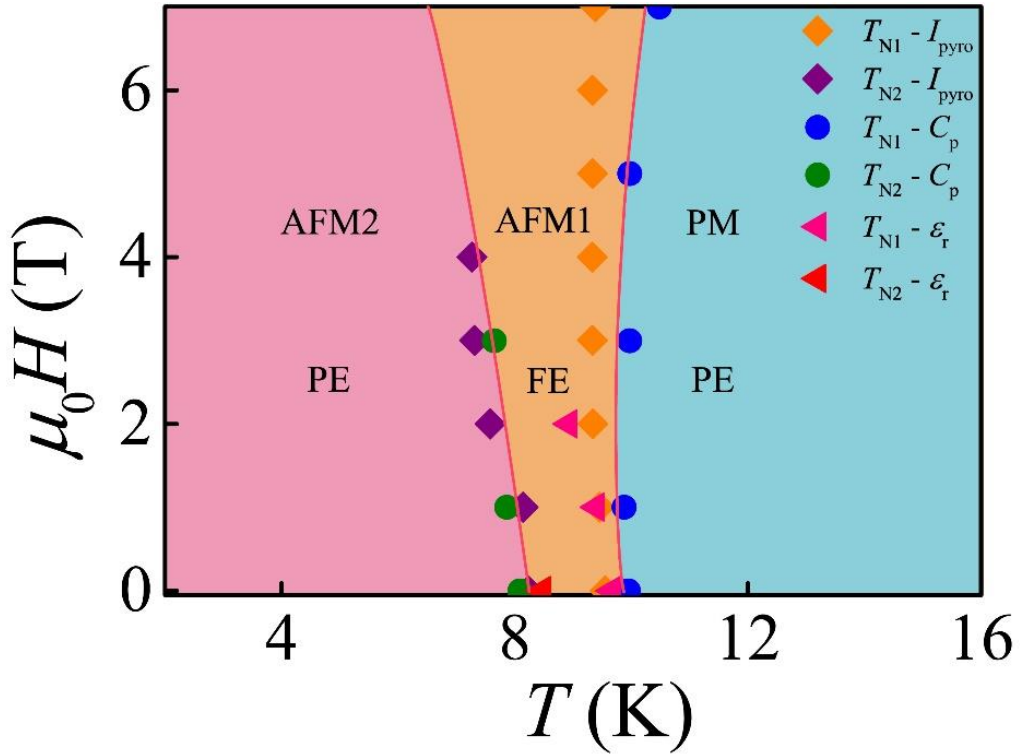


Figure 5. The magnetic and polar phase diagram for $\text{LiCuFe}_2(\text{VO}_4)_3$ determined by aforementioned measurements. The multiferroic phase exists only in the intermediate window.

V. CONCLUSION

In summary, we have systematically investigated the magnetism and multiferroicity in mixed spin chain $\text{LiCuFe}_2(\text{VO}_4)_3$. Magnetic susceptibility and specific heat showed two adjacent AFM transitions at $T_{\text{N1}} \sim 9.95$ K and $T_{\text{N2}} \sim 8.17$ K. Pyroelectric current and dielectric measurements confirmed that the FE transition at T_{N1} . Interestingly, two sign-opposite pyroelectric peaks are observed at T_{N1} and T_{N2} , giving rise to a reentrant paraelectric phase below T_{N2} . Moreover, the FE P of $\text{LiCuFe}_2(\text{VO}_4)_3$ is very sensitive to magnetic fields, i.e., it exhibits significant ME effect. We suggest that the sequential magnetic transitions lead to this special multiferroic behavior, namely only the intermediate AFM1 phase can induce polarization. Further studies using single crystal samples and neutron experiments are encouraged to verify our proposal of multiferroicity in $\text{LiCuFe}_2(\text{VO}_4)_3$.

ACKNOWLEDGMENTS

This work was supported by the National Natural Science Foundation of China (Grant Nos. 11834002, 12074111, 92163210, 11704109). The Research Project of Hubei Provincial Department of Education (Grant No. Q20202502).

References

1. Dong, S.; Liu, J.-M.; Cheong, S.-W.; Ren, Z., Multiferroic materials and magnetoelectric physics: symmetry, entanglement, excitation, and topology. *Adv. Phys.* **2015**, *64*, 519-626.
2. Fiebig, M.; Lottermoser, T.; Meier, D.; Trassin, M., The evolution of multiferroics. *Nat. Rev. Mater.* **2016**, *1*, 16046.
3. Dong, S.; Xiang, H.; Dagotto, E., Magnetoelectricity in multiferroics: a theoretical perspective. *Natl. Sci. Rev.* **2019**, *6*, 629-641.
4. Spaldin, N. A.; Ramesh, R., Advances in magnetoelectric multiferroics. *Nat. Mater.* **2019**, *18*, 203-212.
5. Lu, C.; Wu, M.; Lin, L.; Liu, J.-M., Single-phase multiferroics: new materials, phenomena, and physics. *Natl. Sci. Rev.* **2019**, *6*, 653-668.
6. Schoenherr, P.; Manz, S.; Kuerten, L.; Shapovalov, K.; Iyama, A.; Kimura, T.; Fiebig, M.; Meier, D., Local electric-field control of multiferroic spin-spiral domains in TbMnO₃. *npj Quantum Mater.* **2020**, *5*, 86.
7. Kimura, K.; Kato, Y.; Kimura, S.; Motome, Y.; Kimura, T., Crystal-chirality-dependent control of magnetic domains in a time-reversal-broken antiferromagnet. *npj Quantum Mater.* **2021**, *6*, 54.
8. Cheong, S. W.; Mostovoy, M., Multiferroics: a magnetic twist for ferroelectricity. *Nat. Mater.* **2007**, *6*, 13-20.
9. Khomskii, D., Classifying multiferroics: Mechanisms and effects. *Physics* **2009**, *2*, 20.
10. Sergienko, I. A.; Dagotto, E., Role of the Dzyaloshinskii-Moriya interaction in multiferroic perovskites. *Phys. Rev. B* **2006**, *73*, 094434.
11. Murakawa, H.; Onose, Y.; Miyahara, S.; Furukawa, N.; Tokura, Y., Ferroelectricity Induced by Spin-Dependent Metal-Ligand Hybridization in Ba₂CoGe₂O₇. *Phys. Rev. Lett.* **2010**, *105*, 137202.
12. Murakawa, H.; Onose, Y.; Miyahara, S.; Furukawa, N.; Tokura, Y., Comprehensive study of the ferroelectricity induced by the spin-dependent hybridization mechanism in Ba₂XGe₂O₇ (X= Mn, Co, and Cu). *Phys. Rev. B* **2012**, *85*, 174106.
13. Choi, Y. J.; Yi, H. T.; Lee, S.; Huang, Q.; Kiryukhin, V.; Cheong, S. W., Ferroelectricity in

- an Ising Chain Magnet. *Phys. Rev. Lett.* **2008**, 100, 047601.
14. Wu, H.; Burnus, T.; Hu, Z.; Martin, C.; Maignan, A.; Cezar, J. C.; Tanaka, A.; Brookes, N. B.; Khomskii, D. I.; Tjeng, L. H., Ising Magnetism and Ferroelectricity in $\text{Ca}_3\text{CoMnO}_6$. *Phys. Rev. Lett.* **2009**, 102, 026404.
 15. Zhang, G.; Dong, S.; Yan, Z.; Guo, Y.; Zhang, Q.; Yunoki, S.; Dagotto, E.; Liu, J. M., Multiferroic properties of $\text{CaMn}_7\text{O}_{12}$. *Phys. Rev. B* **2011**, 84, 174413.
 16. Zhou, L.; Dai, J.; Chai, Y.; Zhang, H.; Dong, S.; Cao, H.; Calder, S.; Yin, Y.; Wang, X.; Shen, X.; Liu, Z.; Saito, T.; Shimakawa, Y.; Hojo, H.; Ikuhara, Y.; Azuma, M.; Hu, Z.; Sun, Y.; Jin, C.; Long, Y., Realization of Large Electric Polarization and Strong Magnetoelectric Coupling in $\text{BiMn}_3\text{Cr}_4\text{O}_{12}$. *Adv. Mater.* **2017**, 29, 1703435.
 17. Wang, X.; Chai, Y.; Zhou, L.; Cao, H.; Cruz, C. D.; Yang, J.; Dai, J.; Yin, Y.; Yuan, Z.; Zhang, S.; Yu, R.; Azuma, M.; Shimakawa, Y.; Zhang, H.; Dong, S.; Sun, Y.; Jin, C.; Long, Y., Observation of Magnetoelectric Multiferroicity in a Cubic Perovskite System: $\text{LaMn}_3\text{Cr}_4\text{O}_{12}$. *Phys. Rev. Lett.* **2015**, 115, 087601.
 18. Liu, M.; Lin, L.; Zhang, Y.; Li, S.; Huang, Q.; Garlea, V. O.; Zou, T.; Xie, Y.; Wang, Y.; Lu, C.; Yang, L.; Yan, Z.; Wang, X.; Dong, S.; Liu, J.-M., Cycloidal magnetism driven ferroelectricity in double tungstate $\text{LiFe}(\text{WO}_4)_2$. *Phys. Rev. B* **2017**, 95, 195134
 19. Wang, Z.; Lorenz, T.; Gorbunov, D. I.; Cong, P. T.; Kohama, Y.; Niesen, S.; Breunig, O.; Engelmayer, J.; Herman, A.; Wu, J.; Kindo, K.; Wosnitza, J.; Zherlitsyn, S.; Loidl, A., Quantum Criticality of an Ising-like Spin-1/2 Antiferromagnetic Chain in a Transverse Magnetic Field. *Phys. Rev. Lett.* **2018**, 120, 207205.
 20. Cui, Y.; Zou, H.; Xi, N.; He, Z.; Yang, Y. X.; Shu, L.; Zhang, G. H.; Hu, Z.; Chen, T.; Yu, R.; Wu, J.; Yu, W., Quantum Criticality of the Ising-like Screw Chain Antiferromagnet $\text{SrCo}_2\text{V}_2\text{O}_8$ in a Transverse Magnetic Field. *Phys. Rev. Lett.* **2019**, 123, 067203.
 21. Bera, A. K.; Lake, B.; Islam, A. T. M. N.; Klemke, B.; Faulhaber, E.; Law, J. M., Field-induced magnetic ordering and single-ion anisotropy in the quasi-one-dimensional Haldane chain compound $\text{SrNi}_2\text{V}_2\text{O}_8$: A single-crystal investigation. *Phys. Rev. B* **2013**, 87, 224423.
 22. Dutton, S. E.; Kumar, M.; Mourigal, M.; Soos, Z. G.; Wen, J. J.; Broholm, C. L.; Andersen,

- N. H.; Huang, Q.; Zbiri, M.; Toft-Petersen, R.; Cava, R. J., Quantum Spin Liquid in Frustrated One-Dimensional LiCuSbO₄. *Phys. Rev. Lett.* **2012**, 108, 187206.
23. Park, S.; Choi, Y. J.; Zhang, C. L.; Cheong, S. W., Ferroelectricity in an $S = 1/2$ Chain Cuprate. *Phys. Rev. Lett.* **2007**, 98, 057601.
24. Schrettle, F.; Krohns, S.; Lunkenheimer, P.; Hemberger, J.; Büttgen, N.; Krug von Nidda, H. A.; Prokofiev, A. V.; Loidl, A., Switching the ferroelectric polarization in the $S = 1/2$ chain cuprate LiCuVO₄ by external magnetic fields. *Phys. Rev. B* **2008**, 77, 144101.
25. Ding, L.; Manuel, P.; Khalyavin, D. D.; Orlandi, F.; Tsirlin, A. A., Unraveling the complex magnetic structure of multiferroic pyroxene NaFeGe₂O₆: A combined experimental and theoretical study. *Phys. Rev. B* **2018**, 98, 094416.
26. Colin, C. V.; Ding, L.; Ressouche, E.; Robert, J.; Terada, N.; Gay, F.; Lejay, P.; Simonet, V.; Darie, C.; Bordet, P.; Petit, S., Incommensurate spin ordering and excitations in multiferroic SrMnGe₂O₆. *Phys. Rev. B* **2020**, 101, 235109.
27. Taniguchi, K.; Abe, N.; Takenobu, T.; Iwasa, Y.; Arima, T., Ferroelectric Polarization Flop in a Frustrated Magnet MnWO₄ Induced by a Magnetic Field. *Phys. Rev. Lett.* **2006**, 97, 097203.
28. Belik, A. A., SYNTHESIS AND CRYSTAL STRUCTURE OF LiCuFe₂(VO₄)₃ BY RIETVELD METHOD. *Mater. Res. Bull.* **1999**, 34, 1973–1980.
29. Drokina, T. V.; Petrakovskii, G. A.; Bayukov, O. A.; Vorotynov, A. M.; Velikanov, D. A.; Molochev, M. S., Synthesis and Structural, Magnetic, and Resonance Properties of the LiCuFe₂(VO₄)₃ Compound. *Phys. Solid State* **2016**, 58, 1981-1988.
30. Koshelev, A. V.; Zakharov, K. V.; Pyatakov, A. P.; Shvanskaya, L. V.; Shakin, A. A.; Volkova, O. S.; Chareev, D. A.; Kamusella, S.; Klauss, H.-H.; Molla, K.; Rahaman, B.; Saha-Dasgupta, T.; Vasiliev, A. N., Spin-Order-Induced Ferroelectricity and Magnetoelectric Effect in LiCuFe₂(VO₄)₃. *Phys. Rev. Applied* **2018**, 10, 034008.
31. Koshelev, A.; Shvanskaya, L.; Volkova, O.; Zakharov, K.; Theuss, F.; Koo, C.; Klingeler, R.; Kamusella, S.; Klauss, H. H.; Kundu, S.; Bachhar, S.; Mahajan, A. V.; Khuntia, P.; Khanam, D.; Rahaman, B.; Saha-Dasgupta, T.; Vasiliev, A., Thermodynamic and resonant properties of mixed spin compounds ACuFe₂(VO₄)₃ (A = Li, Na). *J. Alloys Compd.* **2020**, 842, 155763.

32. Toby, B. H., EXPGUI, a graphical user interface for GSAS. *J. Appl. Crystallogr.* **2001**, 34, 210.
33. Toby, B. H.; Von Dreele, R. B., GSAS-II: the genesis of a modern open-source all purpose crystallography software package. *J. Appl. Crystallogr.* **2013**, 46, 544-549.
34. He, Z.; Taniyama, T.; Kyômen, T.; Itoh, M., Field-induced order-disorder transition in the quasi-one-dimensional anisotropic antiferromagnet $\text{BaCo}_2\text{V}_2\text{O}_8$. *Phys. Rev. B* **2005**, 72, 172403.
35. Liu, M.; Zhang, H.; Huang, X.; Ma, C.; Dong, S.; Liu, J. M., Two-Step Antiferromagnetic Transitions and Ferroelectricity in Spin-1 Triangular-Lattice Antiferromagnetic $\text{Sr}_3\text{NiTa}_2\text{O}_9$. *Inorg. Chem.* **2016**, 55, 2709-16.
36. Hwang, J.; Choi, E. S.; Ye, F.; Dela Cruz, C. R.; Xin, Y.; Zhou, H. D.; Schlottmann, P., Successive Magnetic Phase Transitions and Multiferroicity in the Spin-One Triangular-Lattice Antiferromagnet $\text{Ba}_3\text{NiNb}_2\text{O}_9$. *Phys. Rev. Lett.* **2012**, 109, 257205.
37. Du, K.; Guo, L.; Peng, J.; Chen, X.; Zhou, Z.-N.; Zhang, Y.; Zheng, T.; Liang, Y.-P.; Lu, J.-P.; Ni, Z.-H.; Wang, S.-S.; Van Tendeloo, G.; Zhang, Z.; Dong, S.; Tian, H., Direct visualization of irreducible ferroelectricity in crystals. *npj Quantum Mater.* **2020**, 5, 49.
38. Higashiyama, D.; Miyasaka, S.; Tokura, Y., Magnetic-field-induced polarization and depolarization in HoMn_2O_5 and ErMn_2O_5 . *Phys. Rev. B* **2005**, 72, 064421.
39. Hur, N.; Park, S.; Sharma, P. A.; Ahn, J. S.; Guha, S.; Cheong, S. W., Electric polarization reversal and memory in a multiferroic material induced by magnetic fields. *Nature* **2004**, 429, 392-5.
40. Higashiyama, D.; Miyasaka, S.; Kida, N.; Arima, T.; Tokura, Y., Control of the ferroelectric properties of DyMn_2O_5 by magnetic fields. *Phys. Rev. B* **2004**, 70, 174405.
41. Zhang, N.; Guo, Y. Y.; Lin, L.; Dong, S.; Yan, Z. B.; Li, X. G.; Liu, J. M., Ho substitution suppresses collinear Dy spin order and enhances polarization in DyMnO_3 . *Appl. Phys. Lett.* **2011**, 99, 102509.
42. Zhang, N.; Dong, S.; Zhang, G. Q.; Lin, L.; Guo, Y. Y.; Liu, J. M.; Ren, Z. F., Multiferroic phase diagram of Y partially substituted $\text{Dy}_{1-x}\text{Y}_x\text{MnO}_3$. *Appl. Phys. Lett.* **2011**, 98, 012510.
43. Zhao, Z. Y.; Liu, M. F.; Li, X.; Lin, L.; Yan, Z. B.; Dong, S.; Liu, J. M., Experimental

observation of ferrielectricity in multiferroic DyMn_2O_5 . *Sci Rep* **2014**, 4, 3984.

44. Liu, J. M.; Dong, S., Ferrielectricity in DyMn_2O_5 : A golden touchstone for multiferroicity of RMn_2O_5 family. *J. Adv. Dielect* **2015**, 05, 1530003.

45. Arkenbout, A. H.; Palstra, T. T. M.; Siegrist, T.; Kimura, T., Ferroelectricity in the cycloidal spiral magnetic phase of MnWO_4 . *Phys. Rev. B* **2006**, 74, 184431.

46. Lawes, G.; Harris, A. B.; Kimura, T.; Rogado, N.; Cava, R. J.; Aharony, A.; Entin-Wohlman, O.; Yildirim, T.; Kenzelmann, M.; Broholm, C.; Ramirez, A. P., Magnetically Driven Ferroelectric Order in $\text{Ni}_3\text{V}_2\text{O}_8$. *Phys. Rev. Lett.* **2005**, 95, 087205.

47. Kimura, T.; Sekio, Y.; Nakamura, H.; Siegrist, T.; Ramirez, A. P., Cupric oxide as an induced-multiferroic with high- T_C . *Nat. Mater.* **2008**, 7, 291-4.

48. Wang, Z.; Qureshi, N.; Yasin, S.; Mukhin, A.; Ressouche, E.; Zherlitsyn, S.; Skourski, Y.; Geshev, J.; Ivanov, V.; Gospodinov, M.; Skumryev, V., Magnetoelectric effect and phase transitions in CuO in external magnetic fields. *Nat. Commun.* **2016**, 7, 10295.

49. Taniguchi, K.; Abe, N.; Ohtani, S.; Arima, T., Magnetoelectric memory effect of the nonpolar phase with collinear spin structure in multiferroic MnWO_4 . *Phys. Rev. Lett.* **2009**, 102, 147201.

50. Wu, W. B.; Huang, D. J.; Okamoto, J.; Huang, S. W.; Sekio, Y.; Kimura, T.; Chen, C. T., Multiferroic nanoregions and a memory effect in cupric oxide. *Phys. Rev. B* **2010**, 81, 172409.